Chin. Sci. Bull. (2014) 59(3):310–319
DOI 10.1007/s11434-013-0038-z

Evolution of stomatal and trichome density of the *Quercus delavayi* complex since the late Miocene

Qian Hu · Yaowu Xing · Jinjin Hu · Yongjiang Huang · Hongjie Ma · Zhekun Zhou

Received: 12 December 2012 / Accepted: 18 February 2013 / Published online: 31 December 2013

Abstract A fossil oak species, *Quercus tenuipilosa* Q. Hu et Z.K. Zhou, is reported from the upper Pliocene Ciying Formation in Kunming, Yunnan Province, southwestern China. The establishment of this species is based on detailed morphologic and cuticular investigations. The fossil leaves are elliptic, with serrate margins on the apical half. The primary venation is pinnate, and the major secondary venation is craspedodromous. The tertiary veins are opposite or alternate-opposite percurrent with two branches. The stomata are anomocytic, occurring only on the abaxial epidermis. The trichome bases are unicellular or multicellular. The new fossil species shows the closest affinity with the extant *Q. delavayi* and the late Miocene *Q. praedelavayi* Y.W. Xing et Z.K. Zhou from the Xiaolongtan Formation of the Yunnan Province. All three species share similar leaf morphology, but differ with respect to trichome base and stomatal densities. *Q. tenuipilosa*, *Q. praedelavayi*, and *Q. delavayi* can be considered to constitute the *Q. delavayi* complex. Since the late Miocene, a gradual reduction in trichome base density has occurred in this complex. This trend is the opposite of that of precipitation, indicating that increased trichome density is not an adaptation to dry environments. The stomatal density (SD) of the *Q. delavayi* complex was the highest during the late Miocene, declined in the late Pliocene, and then increased during the present epoch. These values show an inverse relationship with atmospheric CO_2 concentrations, suggesting that the SD of the *Q. delavayi* complex may be a useful proxy for reconstruction of paleo-CO_2 concentrations.

Keywords *Quercus delavayi* complex · *Quercus tenuipilosa* · Morphology evolution · Neogene · CO_2 concentration

Q. Hu · J. Hu · Y. Huang · Z. Zhou
Key Laboratory of Biogeography and Biodiversity, Kunming Institute of Botany, Chinese Academy of Sciences, Kunming 650201, China

Q. Hu · J. Hu
University of Chinese Academy of Sciences, Beijing 100049, China

Y. Xing (✉) · Z. Zhou (✉)
Key Laboratory of Tropical Forest Ecology, Xishuangbanna Tropical Botanical Garden, Chinese Academy of Sciences, Mengla 666303, China
e-mail: ywxing@xtbg.org.cn

Z. Zhou
e-mail: zhouzk@xtbg.ac.cn

Y. Xing
Institute of Systematic Botany, University of Zürich, 8008 Zürich, Switzerland

H. Ma
Faculty of Land Resource Engineering, Kunming University of Science and Technology, Kunming 650093, China

Plant morphology is determined by the interactions between genetic and environmental factors. Understanding the impact of environmental change on plant traits is an important issue in evolutionary biology. As the only direct evidence of past life, fossils provide important information on the interactions between plants and environmental change. For instance, ''xeromorphic'' cuticular features such as epidermal trichomes, sunken stomata, and stomatal furrows are commonly considered as adaptations to aridity, increasing the boundary layer resistance and consequently limiting transpiration [1, 2]. By comparing the traits of closely related fossil species from different geological periods, we can better understand the responses of plant traits to environmental change [3–6].

Growing plants in artificially controlled environments is the most common method to study the responses of plant traits to environmental change. By this method, Beerling and Woodward found that the stomatal densities and indices of *Hedera helix* L. and *Chlorophytum comosum* (Thunb.) Baker decreased with the doubling of the CO_2 concentration [7]. Another method is to compare traits of the same species from different climatic conditions instead of controlling the environmental factors artificially. By investigating the stomatal density (SD) of *Nothofagus soladri* (Hook. f.) Oerst., Kouwenberg et al. [8] found a positive relationship between SD and elevation along altitudinal gradients. As the concentration of CO_2 decreases when the elevation increases, the SD of *N. soladri* is negatively correlated with CO_2 concentration. On the other hand, Zhou et al. [9] and Hu and Zhou [10] indicated that the SD of *Quercus pannosa* Hand.-Mazz. is positively associated with CO_2 concentration. Another widely used method to investigate the response of plant morphology to climatic change across a large scale is to compare closely related fossils from different geological periods. Franks and Beerling [11] studied the relationship between the stomatal size, intensity, and inductance of plants belonging to the same group from different time periods in relationship to the atmospheric CO_2 concentration. The results showed that the atmospheric CO_2 concentration is the main factor driving the evolution of stomatal conductance [11]. This method gives direct evidence as to how plant traits correspond with climatic change. However, few studies have been carried out, as most groups lack such a complete fossil record.

Quercus subgen. *Cyclobalanopsis* Oerst. (Fagaceae) are evergreen trees mainly occurring in subtropical to tropical regions in East and South Eastern Asia [12–15]. China is a major center of diversity for subgen. *Cyclobalanopsis* and contains 69 species, which represents 62 % of the total species from all over the world, and are often found as dominant elements in subtropical to tropical broad-leaved evergreen forests [14]. *Q.* subgen. *Cyclobalanopsis* has an abundant fossil record in East Asia during the Cenozoic [16–19]. In Yunnan Province, *Cyclobalanopsis* fossil records are also rich starting in the Oligocene period, including impressions, compressions, and fossil fruits [18–20]. These fossils are comparable with extant species making them suitable to study the evolution of traits in different geological periods.

In this study, we describe a new *Quercus* species from the Pliocene Ciying Formation based on well preserved fossil leaves. The fossil species is comparable with extant *Q. delavayi* and *Q. praedelavayi* Y.W. Xing et Z.K. Zhou from the Late Miocene Xiaolongtan Formation in gross morphology, but differs from these two species in stomatal and trichome densities. We consider these three species as the *Q. delavayi* complex. Based on detailed comparisons of the SD and the trichome density of the *Q. delavayi* complex, we discuss the evolution of the micromorphology of the *Q. delavayi* complex in relation to the changing environment.

1 Materials and methods

1.1 Materials

The fossils were collected from the Pliocene Ciying Formation exposed at Hunshuitang county, located ca. 25 km northeast of Kunming, the capital city of Yunnan Province, southwestern China (Fig. 1). The Ciying Formation can be divided into two parts. The lower layer is composed of gray sandstone, and the upper layer is composed of silty mudstone and sandstone [21]. Current fossils were found in the upper member of the Ciying Formation, which also yields abundant fossil plants and shells. Based on the lithological sequences, the Ciying Formation was considered as belonging to the late Pliocene age [22–24].

Specimens of extant *Quercus delavayi* for comparison are from Herbarium of Kunming Institute of Botany, Chinese Academy of Sciences KUN. The specimens used for epidermis analysis were collected by M. Deng and J.J. Hu in 2010 (Table 1).

The descriptions of Xing et al. [19] of the late Miocene *Quercus praedelavayi* fossils from the Xiaolongtan Formation of Xundian, Yunnan were used. Information on the studied specimens is gathered in Table 1.

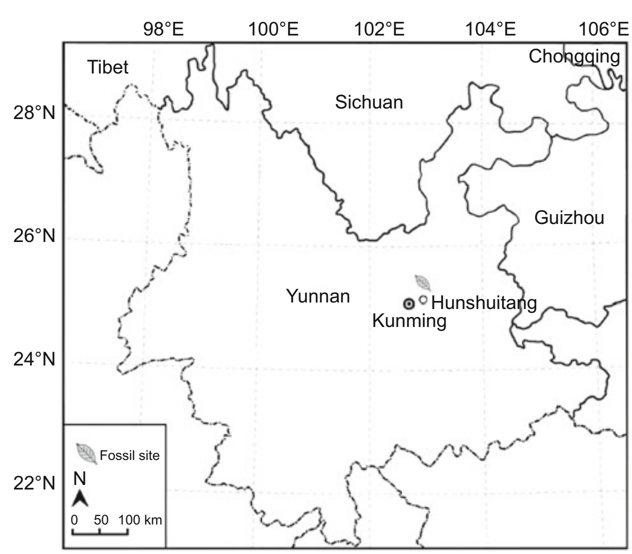

Fig. 1 Map showing the fossil locality (leaf) of *Quercus tenuipilosa*

Table 1 The voucher information of fossils and extant species

Voucher no.	Locality	Age	Coordinates	Altitude (m)	Year of collection
HLT450	Kunming	Late Miocene	N25°25′, E102°51′	2,200	2007
HST856	Kunming	Late Pliocene	N25°06′, E102°57′	2,102	2010
DH008	Jingdong	Extant	N24°26′, E100°54′	1,431	2010
DH020	Binchuan	Extant	N25°54′, E100°25′	1,862	2010
DH025	Binchuan	Extant	N25°57′, E100°22′	2,630	2010
DH029	Binchuan	Extant	N25°57′, E100°22′	2,480	2010
DH030	Binchuan	Extant	N25°56′, E100°24′	2,050	2010
DH032	Eryuan	Extant	N26°19′, E099°59′	2,300	2010
DH034	Jianchuan	Extant	N26°22′, E099°58′	2,541	2010
DH037	Lijiang	Extant	N26°38′, E099°57′	2,274	2010
DH044	Lijiang	Extant	N26°53′, E100°14′	2,442	2010
DH067	Lijiang	Extant	N26°52′, E100°01′	2,159	2010
DH074	Eryuan	Extant	N25°56′, E099°49′	1,932	2010
DH075	Eryuan	Extant	N25°54′, E099°49′	1,763	2010
DH076	Yangbi	Extant	N25°50′, E099°53′	1,689	2010
KUN0094673	Jinggu	Extant	?	1,600	?
KUN0396795	Zhongdian	Extant	?	1,900	1981
KUN0396899	Weixi	Extant	?	1,920	1981
KUN0449347	Fumin	Extant	?	1,670	?
KUN0449364	Jiangchuan	Extant	?	1,950	1989
KUN0449366	Heqing	Extant	?	1,900	?
KUN0449389	Songming	Extant	?	1,920	1956
KUN0449391	Shuangbai	Extant	?	2,090	?
KUN0449397	Kunming	Extant	?	1,035	1942
KUN0468641	Lufeng	Extant	?	1,900	1982
KUN0504244	Yanshan	Extant	?	1,200	?

? means unknown

Table 2 Comparison of the leaf macro- and micro- morphology of *Quercus tenuipilosa* with its closely related species

Species and references	Age	Gross morphology					Micro-morphology		
		L:*W*	*N*	*P*	*S*	*T*	*U&M*	*TD* (n mm^{-2})/*TI* (%)	*SD* (n mm^{-2})/*SI* (%)
Quercus praedelavayi [19]	Late Miocene	3	13–15	+	+	+	~	282/?	1,139/?
Q. aff. *delavayi* [37]	Late Miocene	4	10	~	~	+	+	192/5.2	465/11.7
Q. tenuipilosa	Late Pliocene	2.5	13	+	+	+	+	250/10.2	672/19.1
Q. delavayi [14]	Extant	2.8–4	10–14	+	+	+	+	194/3.6	931/15.2

L leaf length, *W* leaf width, *N* number of pairs of secondaries, *P* straight primary vein, *S* secondary vein alternate, *T* tertiary vein branch, *U&M* unicellular and multicellular trichome bases on the adaxial epidermis, *TD* trichome density on the abaxial epidermis, *TI* trichome index on the abaxial epidermis, *SD* stomatal density on the abaxial epidermis, *SI* stomatal index on the abaxial epidermis, + yes, ~ no, ? unknown

1.2 Methods

(1) *Epidermis characteristics of the fossil species* The procedure of making fossil epidermis slides followed the methods of Ye [25], Leng [26], and Ma et al. [27].

(2) *Epidermis characteristics of the extant Quercus delavayi* We followed the method of Stace to make the epidermis slides of extant *Q. delavayi* [3].

(3) *Making cleared leaves* For the examination of the leaf morphology of extant subgen. *Cyclobalanopsis* leaves, we followed the methods of Hickey and Wolfe [28] to make cleared leaves (Table 2).

(4) *Trichome density* Instead of counting trichomes directly, the trichome bases were counted. Three visual fields under 20× magnification were used to calculate the trichome density (Table 2).

Table 3 The taxon-characteristic matrix for the PCoA analysis

Characters	Species			
	Quercus praedelavayi [19]	*Q.* aff. *delavayi* [37]	*Q. tenuipilosa*	Extant *Q. delavayi* [14]
Lanceolate leaf	0	1	0	0
Elliptic leaf	1	0	1	1
Leaf length ≥10 cm	1	0	0	1
Leaf width ≥2 cm	1	0	1	1
Length:width <5	1	0	1	1
Number of secondary pairs >10	1	0	1	1
Primary vein straight	1	0	1	1
Secondaries alternate and opposite	1	0	1	1
Trichomes on adaxial epidermis	0	1	1	1
Anomocytic stomata	1	1	1	1
Uni- and multi-cellular trichome bases	0	0	1	1
Trichome density <200 n mm^{-2}	0	1	0	1
SD <500 n mm^{-2}	0	1	0	0
SD >1,000 n mm^{-2}	1	0	0	0

(5) SD The same method which was used for counting trichome density was used to determine SD.

(6) *Principal Coordinates analysis (PCoA)* The PCoA is a method to explore and to visualize similarities or dissimilarities between data. The PCoA usually starts with a symmetric distance matrix and assigns for each item a location in a low-dimensional space [29, 30]. In this study, a taxa-characteristic matrix, including four fossil taxa plus the extant *Quercus delavayi*, and 14 characteristics were built and provided (Table 3). The PCoA was carried out using the MultiVariate Statistical Package (MVSP) software [31] and Euclidean distances after the data were standardized.

For descriptions of the leaf morphology and cuticles, we followed the terms of Dilcher [32], Luo and Zhou [33], and Ellis et al. [34].

2 Results

2.1 Systematics

Family: Fagaceae Hand.-Mazz., 1929
Genus: *Quercus* L., 1753
Subgenus: *Cyclobalanopsis* Oerst.

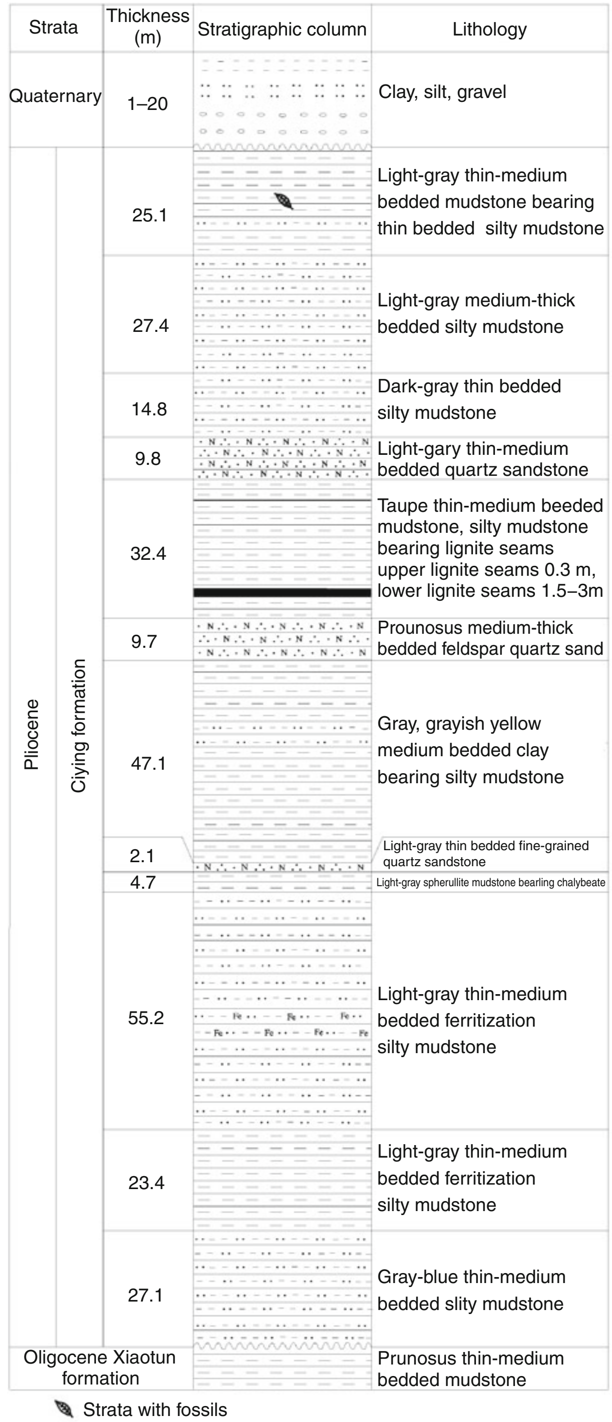

Fig. 2 The sketch strata table of the Ciying Formation. The layer where the fossils were collected is marked with a *leaf symbol*. The figure is compiled from information from the Geological Bureau of Yunnan [21]

Species: *Quercus tenuipilosa* Q. Hu et Z.K. Zhou.

Etymology: The specific epithet *tenuipilosa* represents the rare trichomes of this species. In Latin, *tenuis* means ''thin'' or ''weak'', while *pilosa* means ''hair'' or ''trichome'' (Fig. 2).

Holotype: HST 856 A, B (counterparts) (Fig. 3a, b, e, and g)

Paratype: HST 022 (Fig. 4c)

Other specimens: HST 151, HST 254, HST 565, HST 943A, and HST 943B (Fig. 4a, b, d–f)

Repository: All specimens examined are deposited in KUN.

2.2 Diagnosis

Leaves elliptic, symmetric; leaf apex acuminate and leaf base convex to broadly cuneate. Secondaries in the toothed portion craspedodromous, secondaries in the entire portion are camptodromous; tertiary veins opposite and alternate percurrent. Stomata on the abaxial epidermis, anomocytic. Trichome bases on the adaxial and abaxial epidermis, unicellular and multicellular.

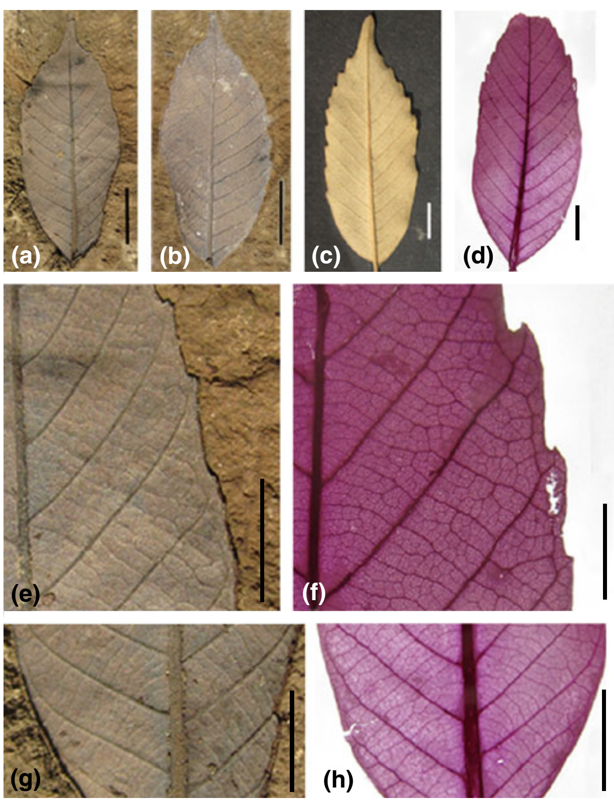

Fig. 3 Comparison of the leaf morphology of *Quercus tenuipilosa* and the extant *Q. delavayi*. **a**, **b** *Quercus tenuipilosa*. Specimen no. HST856A, HST856B. *Scale bars* 1 cm. **c** *Q. delavayi*, DH037. *Scale bar* 1 cm. **d** Clear leaf of *Q. delavayi*. *Scale bar* 1 cm. **e** Close up of the upper portion of the fossil leaf. Specimen no. HST856A. *Scale bar* 1 cm. **f** Close up of the upper portion of the *Q. delavayi* leaf. *Scale bar* 0.5 cm. **g** Close up of the lower portion of the fossil leaf. Specimen no. HST856A. *Scale bar* 0.5 cm. **h** Close up of the lower portion of the *Q. delavayi* leaf. *Scale bar* 0.5 cm

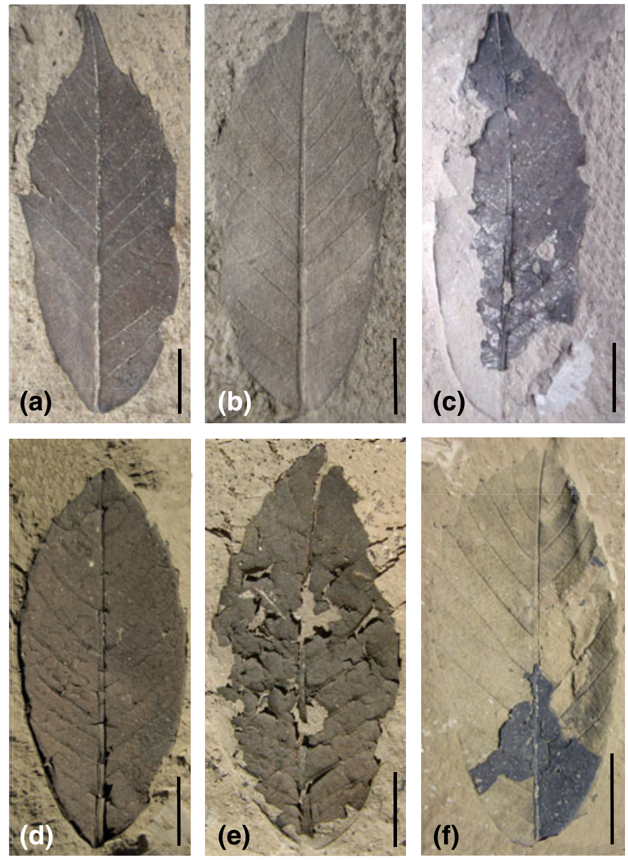

Fig. 4 The paratype and other specimens of *Quercus tenuipilosa*. **a**–**f** HST943A, HST943B, HST022, HST151, HST254, and HST565. *Scale bars* 1 cm

2.3 Description

(1) *Gross morphology* (Figs. 3, 4) Fossil blades are symmetric and elliptic in shape (Fig. 3a, b). The laminar size is 5.0 cm long, 2.0 cm wide (L:$W \approx 2.5$). The blade apex is acuminate. The blade base shape is convex to broadly cuneate. The venation is pinnate with a straight and robust midvein. There are 13 pairs of secondary veins with regular spacing (Fig. 3a, b, e, and g). The major secondaries in the toothed portion are craspedodromous. The secondaries in the entire portion are camptodromous (Fig. 3e, g). The tertiary veins are both opposite and alternate, the outmost tertiaries are looped, running along the margin (Fig. 3e).

(2) *Micromorphology* (Fig. 5) The upper epidermis is composed of quadrangle to hexagonal cells. There are unicellular and multicellular trichome bases (Fig. 5a). The unicellular trichome bases are round, and the multicellular trichome bases are composed of 5–7 cells (Fig. 5a). Stomata are not found in the upper epidermis. The shape of cells in the lower epidermis

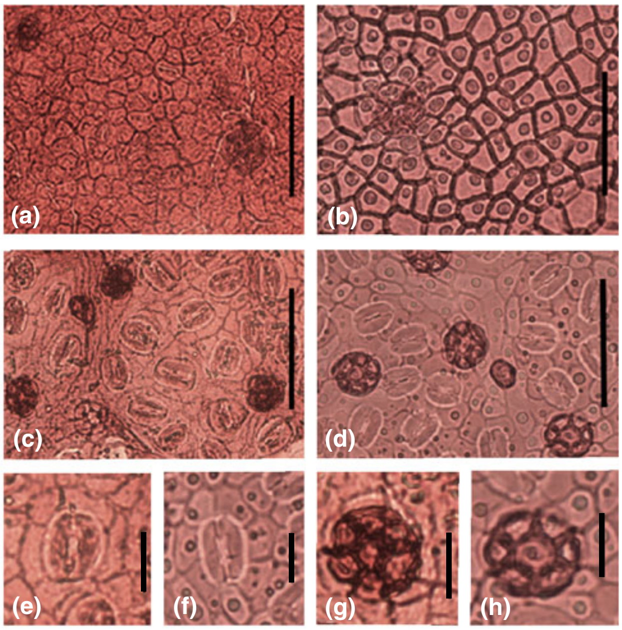

Fig. 5 Cuticular structures of *Quercus tenuipilosa* sp. nov. and *Q. delavayi* under the light microscope. **a** Adaxial epidermis of *Q. tenuipilosa.* Holotype. Slide No. HST856-20120814-upper-01. *Scale bar* 50 μm. **b** Adaxial epidermis of *Q. delavayi.* Slide No. DH030-3A-1. *Scale bar* 50 μm. **c** Abaxial epidermis of *Q. tenuipilosa.* Holotype. Slide No. HST856-20120814-lower-01. *Scale bar* 50 μm. **d** Abaxial epidermis of *Q. delavayi.* Slide No. DH030-4A-2. *Scale bar* 50 μm. **e** Anomocytic stomata of *Q. tenuipilosa. Scale bar* 10 μm. **f** Anomocytic stomata of *Q. delavayi.* Slide No. DH030-4A-2. *Scale bar* 10 μm. **g** Multicellular trichome base of *Q. tenuipilosa.* Slide No. HST856-20120814-lower-01. *Scale bar* 10 μm. **h** Multicellular trichome base of *Q. delavayi.* Slide No. DH030-4A-2. *Scale bar* 10 μm

is irregular (Fig. 5c). The density of the multicellular bases is 250 n mm^{-2} in the lower epidermis. The stomatal apparatuses are elliptical and randomly distributed in the areoles. A single ring of 5–8 subsidiary cells enclosing the two guard cells forms the ananomocytic type (Fig. 5c, g). The SD is ca. 672 n mm^{-2}.

3 Discussion

3.1 Systematic position of the fossil species

Jones [35] studied the leaf morphology and epidermis features of Fagaceae and related families and supplied a framework to identify fagaceous leaves. According to his results, our fossils differ from Juglandaceae by having symmetric bases and differ from Betulaceae by the absence of doubly serrate margins. The synthetic morphologic characteristics of our fossils, such as the symmetric leaf base, possessing unicellular trichome bases, serrate but not doubly serrate, clearly place our fossils into Fagaceae. In the Fagaceae, only *Lithocarpus* and the *Quercus* subgenus *Cyclobalanopsis* possess the same secondary veins as our fossils [33]. However, *Lithocarpus* leaves are usually entire or only partly toothed [35], and most *Lithocarpus* possess a cuneate leaf base rather than the convex base [14]. In China, only eight *Lithocarpus* species are serrated [14], but they differ from our fossils by having larger leaves, with many more secondaries. Thus, our fossils are assigned to the *Quercus* subgenus *Cyclobalanopsis*. We compared our fossils with all extant *Cyclobalanopsis* species in China using the characters listed in Deng [36] and Xing et al. [19]. We found that our fossils are similar to *Q. glauca*, *Q. schottkyana*, and *Q. delavayi*. However, the fossil species has both unicellular and multicellular trichome bases, while *Q. glauca* and *Q. schottkyana* only have unicellular trichome bases on the abaxial epidermis [19]. Thus, the fossil species is most similar to the extant *Q. delavayi*.

Until now, several fossil species have shown a close affinity with the extant *Q. delavayi* including *Q.* aff. *delavayi* from the late Miocene Tiantai flora, Zhejiang Province [37] and *Q. praedelavayi* from the late Miocene Xianfeng flora, Yunnan Province [19]. Among these fossil species, *Q.* aff. *delavayi* possesses much narrower leaves than our fossils with *L*:*W* >5, and *Q. praedelavayi* is very similar to our fossils in the leaf architecture but differs from our fossils by possessing larger leaves and lacking trichome bases on the adaxial epidermis (Table 2). *Q. praedalavayi*, *Q.* aff. *delavayi*, and our fossils share similar epidermis characteristics such as cell shape and trichome base type. However, our fossils and *Q.* aff. *delavayi* possess both unicellular and multicellular trichome bases on the adaxial epidermis, while *Q. praedelavayi* does not possess trichome bases on the adaxial epidermis [19]. *Q.* aff. *delavayi* and *Q. praedelavayi* also differ from our fossils in the trichome and stomatal densities (Table 2). To explore the similarities between our fossils and the other two fossil species and the extant *Q. delavayi*, we carried out the PCoA using 14 characteristics (Table 3; Fig. 3). The results indicated that *Q.* aff. *delavayi* is distinct from the other three species. Our fossils are most similar to the extant *Q. delavayi*, followed by *Q. praedelavayi*. Considering the differences in trichome and stomatal densities, we describe it as a new fossil species, *Q. tenuipilosa*. As *Q. tenuipilosa* and *Q. praedelavayi* both show close affinity with *Q. delavayi*, they could be considered as part of the *Q. delavayi* complex.

3.2 Evolution of the trichome density of the *Quercus delavayi* complex

Epidermal trichomes, sunken stomata, and stomatal furrows are commonly considered as adaptations to aridity, increasing the boundary layer resistance and consequently

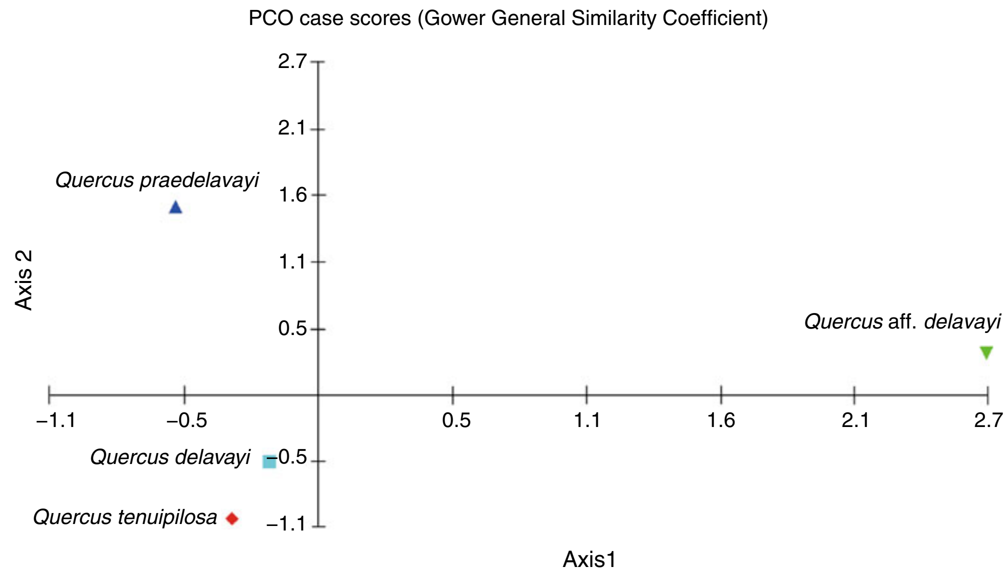

Fig. 6 The morphologic principal coordinates analysis (PCoA) based on 14 characteristics of *Quercus tenuipilosa* and related species

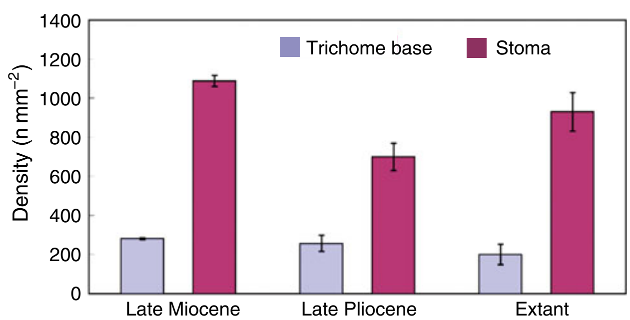

Fig. 7 The trichome density and SD of the *Quercus delavayi* complex

limiting transpiration [1, 2, 38, 39]. However, many plants in humid regions also have trichomes [40]. Previous studies have indicated that trichomes may have other functions, such as anti-herbivory defenses, reducing incident light, and decreasing photosynthetic rates [41, 42].

Hardin studied the seasonal trichome variations of *Quercus* from Eastern North America and found the trichome density of *Quercus* was affected by environmental change [43]. Levin demonstrated that the morphology and density of trichomes show linear relationships with environmental parameters, but the responses are species-specific [44]. In this study, we showed that the trichome densities of the *Q. delavayi* complex decreased from the Late Miocene to the present epoch (Table 1; Fig. 4). Palaeoclimatic reconstructions suggest that the climate during the Late Miocene in Yunnan was warmer and more humid and became cooler and drier since the Pliocene [45–51]. The relationship between the trichome density of the *Q. delavayi* complex and the palaeoclimate contradict the

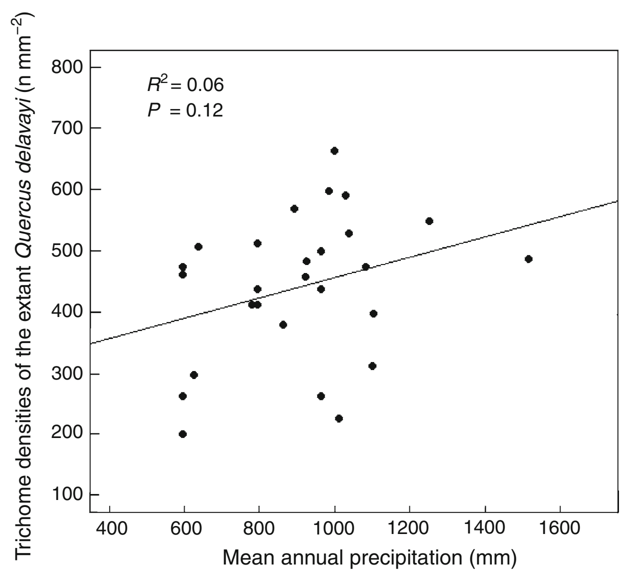

Fig. 8 The regression of the trichome densities of the extant *Quercus delavayi* in relationship to the mean annual precipitation of 27 localities

hypothesis that leaf trichomes are an adaptation to the cooler and drier environment [8, 52]. To further test this hypothesis, we studied the trichome densities of extant *Q. delavayi* from 27 localities and made a regression against the mean annual precipitation. Analysis of the regression results indicated that there is no significant relationship between the trichome density of *Q. delavayi* and local precipitation ($R^2 = 0.0579$, $P = 0.1196$). Haworth et al. [53] also showed that xeromorphic traits are not restricted to plants subjected to water stress but also serve multiple functions such as water-repellence, defense, and protection

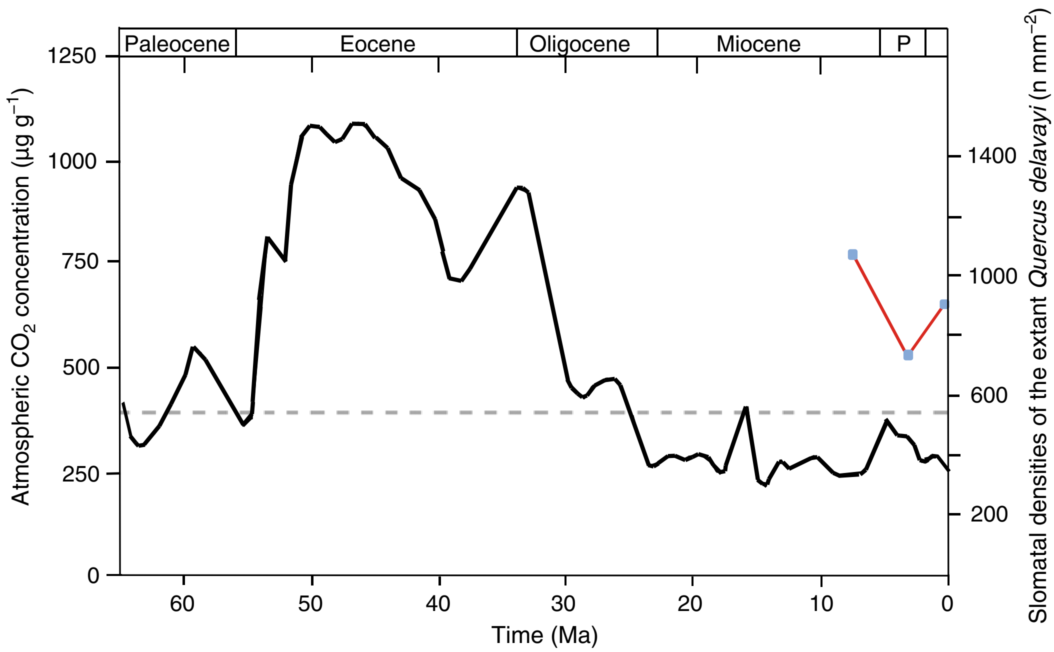

Fig. 9 The Cenozoic CO_2 concentration and the stomatal densities of the *Quercus delavayi* complex. *P* Pliocene

from excess light. Further ecologic and growth experiments are required to fully understand the function of epidermis trichomes.

3.3 Evolution of the SD of the *Quercus delavayi* complex

As a gateway for gas exchange and transpiration of plants, SD, size, and conductance are sensitive to changes in the CO_2 concentration [7, 53–55]. The relationship between SD, stomatal index (SI), and CO_2 concentration change has been investigated intensively, showing either positive or negative responses (e.g., [54, 56]). Royer analyzed the responses of the SD and SI of 176 C3 plants to CO_2 concentration. The results showed that 40 % and 36 % of the species (for SD and SI, respectively) in experimental studies and 88 % and 94 % of the species in fossil studies showed inverse relationships, while <12 % of the species show positive relationships with CO_2 concentration [56]. Haworth measured the SI of six Cupressaceae species and found that the SI of three species (*Tetraclinis articulata*, *Callitris columnaris*, and *C. rhomboidea*) showed significant inverse relationships with rising CO_2, while the other three species (*Athrotaxis cupressoides*, *C. preissii*, and *C. oblonga*) showed no response in SI [53] (Figs. 6, 7, 8).

Furthermore, to test whether CO_2 concentration is the main factor influencing SD and SI, Kouwenberg et al. [8] and Royer [56] discussed the impact of other climatic parameters (temperature, precipitation, and UV-B radiation) on the stomatal frequency, respectively. Their results showed that CO_2 is the most important factor influencing the SD and SI.

In this study, we determined the SD of the *Quercus delavayi* complex from the Late Miocene, the Late Pliocene, and the present epoch (Table 2; Fig. 4). The results indicated that the SD of the *Q. delavayi* complex was the highest during the late Miocene, declined in the late Pliocene, and then increased again at the present epoch. The Cenozoic CO_2 concentrations from these three epochs show the opposite trend. The CO_2 concentration was the lowest in the Late Miocene, increased dramatically during the Pliocene, and dropped again until the present epoch (pre-industrial) [57]. These results indicated that the SD of the *Q. delavayi* complex showed an inverse relationship with atmospheric CO_2 concentrations, suggesting that the SD of the *Q. delavayi* complex may be a good proxy for reconstruction of paleo-CO_2 concentrations (Fig. 9).

Acknowledgments We thank Dr. Frédéric M.B. Jacques for naming the new species, Mr. Guy Atchison for English phrasing, and Dr. Tao Su and Mr. Haobo Wang for their constructive suggestions and help during the field work. This work was supported by the National Basic Research Program of China (2012CB821901), the National Natural Science Foundation of China (41030212) to Zhekun Zhou.

References

1. Axsmith BJ, Jacobs BF (2005) The conifer *Frenelopsis ramosissima* (Cheirolepidiaceae) in the lower cretaceous of texas: systematic, biogeographical, and paleoecological implications. Int J Plant Sci 166:327–337

2. Kunzmann L, Mohr BA, Bernardes-de-Oliveira ME et al (2006) Gymnosperms from the early Cretaceous Crato Formation (Brazil). II. Cheirolepidiaceae. Foss Rec 9:213–222
3. Stace CA (1965) Cuticular studies as an aid to plant taxonomy. Bull Brit Mus (Nat Hist) Bot 4:3–78
4. Beerling DJ, Chaloner WG (1993) The impact of atmospheric CO_2 and temperature changes on stomatal density: observation from *Quercus robur* lammas leaves. Ann Bot 71:231–235
5. McElwain JC, Chaloner WG (1996) The fossil cuticle as a skeletal record of environmental change. Palaios 11:376–388
6. Sun BN, Yan DF, Xie SP et al (2009) General discussion on cuticles of fossil plants in China. Acta Palaeontol Sin 3:347–356
7. Beerling D, Woodward F (1995) Stomatal responses of variegated leaves to CO_2 enrichment. Ann Bot 75:507–511
8. Kouwenberg LL, Kürschner WM, McElwain JC (2007) Stomatal frequency change over altitudinal gradients: prospects for paleoaltimetry. Rev Miner Geochem 66:215–241
9. Zhou ZK, Hu JJ, Su T, et al (2011) Changes in stomatal frequency in two oaks along an elevation gradients in the Himalayas. In: Proceedings of the XVIII international botanical congress, Melbourne
10. Hu JJ, Zhou ZK (2012) The relationship between stomatal frequency and atmospheric pCO_2 of *Quercus pannosa* and its application to paleoelevation reconstruction. Jpn J Palynol 58:91–92
11. Franks PJ, Beerling DJ (2009) Maximum leaf conductance driven by CO_2 effects on stomatal size and density over geologic time. Proc Natl Acad Sci USA 106:10343–10347
12. Hsu Y, Jen H (1976) The classification and distribution of Fagaceae of Yunnan Province (II). Acta Phytotax Sin 14:84–85
13. Zhou ZK (1993) Geographical distribution of *Quercus* from China. J Grad School Acad Sin 10:95–102
14. Huang C, Zhang Y, Bartholomew B (1999) Fagaceae. Flora China 4:314–400
15. Luo Y, Zhou ZK (2001) Phytogeography of *Quercus* subg *Cyclobalanopsis*. Acta Bot Yunnan 23:1–16
16. The Writing Group of Cenozoic Plants of China (1978) Cenozoic plants from China. Science Press, Beijing
17. Zhou ZK (1993) The fossil history of *Quercus*. Acta Bot Yunnan 15:21–33
18. Ge HR, Li DY (1999) Cenozoic coal-bearing basins and coal-forming regularity in West Yunnan. Yunnan Science and Technology Press, Kunming, pp 20–85
19. Xing YW, Hu JJ, Jacques FMB et al (2013) A new *Quercus* species from the Upper Miocene of southwestern China and its ecological significance. Rev Palaeobot Palynol 193:99–109
20. Wen WW (2011) Nine fossil plants of Fagaeeae from the Pliocene in Baoshan, Yunnan and paleoenvironmental analysis. Master's Thesis, Lanzhou University, Lanzhou
21. Geological Bureau of Yunnan. Geological survey of Qujing area, 1:200000 sheet. 1978
22. Compiling Group of Regional Stratigraphic Scale of Yunnan (1978) Regional stratigraphic scale of southwest China: Yunnan Province. Geological Publishing House, Beijing
23. Bureau of Geology (1990) Regional geology of Yunnan province (in Chinese). Geological Publishing House, Beijing
24. Jiang CS, Zhou RQ, Hu YX (2003) Features of geological structure for Kunming basin. J Seismol Res 1:009
25. Ye MN (1981) On the preparation methods of fossil cuticle. In: proceedings of the selected papers of the 12th annual conference of the palaeontogical society of China. Science Press, Beijing
26. Leng Q (2000) An effective method of observing fine venation from compressed angiosperm fossil leaves. Acta Palaeontol Sin 39:158–159
27. Ma QW, Zhang XS, Li FL (2005) Methods of maceration and microscopical analysis on cuticle. Bull Bot Res 25:307–310
28. Hickey LJ, Wolfe JA (1975) The bases of angiosperm phylogeny: vegetative morphology. Ann Mo Bot Garden 62:538–589
29. Gower JC (1966) Some distance properties of latent root and vector methods used in multivariate analysis. Biometrika 53:325–338
30. Anderson MJ (2003) PCO: A fortran computer program for principal coordinate analysis. Department of Statistics, University of Auckland, New Zealand
31. Kovach WL (1998) MVSP: a multivariate statistical package for windows, ver. 3.0. Kovach Computing Services, Pentraeth, Wales. ver.3.0
32. Dilcher DL (1974) Approaches to the identification of angiosperm leaf remains. Bot Rev 40:1–157
33. Luo Y, Zhou ZK (2002) Leaf architecture in *Quercus* subgenus *Cyclobalanopsis* (Fagaceae) from China. Bot J Linn Soc 140:283–295
34. Ellis B, Daly DC, Hickey LJ et al (2009) Manual of leaf architecture. Cornell University Press, Ithaca
35. Jones JH (1986) Evolution of the fagaceae: the implications of foliar features. Ann Mo Bot Garden 73:228–275
36. Deng M (2007) Anatomy, taxonomy, distribution, and phylogeny of *Quercus* subgenus *Cyclobalanopsis* (Oersted) Schneid. (Fagaceae). Doctor Thesis, Chinese Academy of Sciences, Kunming
37. Jia H, Sun BN, Li XC et al (2009) Microstructures of one species of *Quercus* from the Neogene in eastern Zhejiang and its palaeoenvironmental indication. Earth Sci Front 16:79–90
38. Wuenscher JE (1970) The effect of leaf hairs of verbascum thapsus on leaf energy exchange. New Phytol 69:65–73
39. Aronne G, De Micco V (2001) Seasonal dimorphism in the mediterranean *Cistus incanus* L. subsp. *incanus* Ann Bot 87:789–794
40. Wu JY (2009) The Pliocene Tuantian flora of Tengchong, Yunnan province and its paleoenvironmental analysis. Doctor Thesis, Lanzhou University, Lanzhou, p 1–119
41. Haworth M, McElwain J (2008) Hot, dry, wet, cold or toxic? Revisiting the ecological significance of leaf and cuticular micromorphology. Palaeogeogr Palaeoclimatol Palaeoecol 262:79–90
42. McGuire R, Agrawal A (2005) Trade-offs between the shade-avoidance response and plant resistance to herbivores? Tests with mutant cucumis sativus. Funct Ecol 19:1025–1031
43. Hardin JW (1979) Patterns of variation in foliar trichomes of eastern North American *Quercus*. Am J Bot 66:576–585
44. Levin DA (1973) The role of trichomes in plant defense. Q Rev Biol 48:3–15
45. Xia K, Su T, Liu Y-SC et al (2009) Quantitative climate reconstructions of the Late Miocene Xiaolongtan megaflora from Yunnan, southwest China. Palaeogeogr Palaeoclimatol Palaeoecol 276:80–86
46. Jacques F, Guo SX, Su T et al (2011) Quantitative reconstruction of the late Miocene monsoon climates of southwest China: a case study of the Lincang flora from Yunnan Province. Palaeogeogr Palaeoclimatol Palaeoecol 304:318–327
47. Xu JX (2002) Palynology, paleovegetation and paleoclimate of Neogene, central-western Yunnan, China. Doctor Thesis, Chinese Academy of Sciences, Beijing
48. Xing YW, Utescher T, Jacques FMB et al (2012) Paleoclimatic estimation reveals a weak winter monsoon in southwestern China during the late Miocene: evidence from plant macrofossils. Palaeogeogr Palaeoclimatol Palaeoecol 358–360:19–26
49. Li WY, Wu XF (1978) A palynological investigation on the late tertiary and early quarternary and its significance in the paleogeographical study in central Yunnan. Acta Geograph Sin 33:142–155
50. Su T (2010) On the establishment of the leaf physiognomy-climate model and a study of the late Pliocene Yangjie flora,

southwest China. Doctor Thesis, Graduate School of the Chinese Academy of Science, Beijing
51. Huang YJ (2012) The late Pliocene Fudong flora from lanping, Yunnan, and the Neogene climates in Hengduan mountains. Doctor Thesis, Graduate School of the Chinese Academy of Science, Beijing
52. Ehleringer JR (1988) Changes in leaf characteristics of species along elevational gradients in the Wasatch Front, Utah. Am J Bot 75:680–689
53. Haworth M, Heath J, McElwain JC (2010) Differences in the response sensitivity of stomatal index to atmospheric CO_2 among four genera of Cupressaceae conifers. Ann Bot 105:411–418
54. Woodward F (1987) Stomatal numbers are sensitive to increases in CO_2 from pre-industrial levels. Nature 327:617–618
55. Woodward F, Kelly C (1995) The influence of CO_2 concentration on stomatal density. New Phytol 131:311–327
56. Royer D (2001) Stomatal density and stomatal index as indicators of paleoatmospheric CO_2 concentration. Rev Palaeobot Palynol 114:1–28
57. Beerling DJ, Royer DL (2011) Convergent cenozoic CO_2 history. Nat Geosci 4:418–420